Proton-mediated burst of dual-drug loaded liposomes for biofilm dispersal and bacterial killing

Wang, Da Yuan; Yang, Guang; Zhang, Xiao-Xiao; van der Mei, Henny C.; Ren, Yijin; Busscher, Henk J.; Shi, Linqi

Published in:
Journal of Controlled Release

DOI:
10.1016/j.jconrel.2022.10.049

Publication date:
2022

Journal of Controlled Release 352 (2022) 460–471

Contents lists available at ScienceDirect

Journal of Controlled Release

journal homepage: www.elsevier.com/locate/jconrel

Proton-mediated burst of dual-drug loaded liposomes for biofilm dispersal and bacterial killing

Da-Yuan Wang [a,b], Guang Yang [a,b], Xiao-Xiao Zhang [a], Henny C. van der Mei [b,*], Yijin Ren [c], Henk J. Busscher [b,*], Linqi Shi [a,*]

[a] State Key Laboratory of Medicinal Chemical Biology, Key Laboratory of Functional Polymer Materials, Ministry of Education, Institute of Polymer Chemistry, College of Chemistry, Nankai University, Tianjin 300350, PR China
[b] University of Groningen and University Medical Center Groningen, Department of Biomedical Engineering, Antonius Deusinglaan 1, 9713, AV, Groningen, The Netherlands
[c] University of Groningen and University Medical Center Groningen, Department of Orthodontics, Hanzeplein 1, 9700, RB, Groningen, The Netherlands

ARTICLE INFO

Keywords:
Ciprofloxacin
Bromelain
Self-targeting
Dual-drug loaded
Prevention of sepsis
Staphylococcus aureus
In vivo

ABSTRACT

Exposure of infectious biofilms to dispersants induces high bacterial concentrations in blood that may cause sepsis. Preventing sepsis requires simultaneous biofilm dispersal and bacterial killing. Here, self-targeting DCPA (2-(4-((1,5-bis(octadecenoyl)1,5-dioxopentan-2-yl)carbamoyl)pyridin-1-ium-1-yl)acetate) liposomes with complexed water were self-assembled with ciprofloxacin loaded in-membrane and PEGylated as a lipid-membrane component, together with bromelain loaded in-core. Inside biofilms, DCPA-H_2O and PEGylated ciprofloxacin became protonated, disturbing the balance in the lipid-membrane to cause liposome-burst and simultaneous release of bromelain and ciprofloxacin. Simultaneous release of bromelain and ciprofloxacin enhanced bacterial killing in *Staphylococcus aureus* biofilms as compared with free bromelain and/or ciprofloxacin. After tail-vein injection in mice, liposomes accumulated inside intra-abdominal staphylococcal biofilms. Subsequent liposome-burst and simultaneous release of bromelain and ciprofloxacin yielded degradation of the biofilm matrix by bromelain and higher bacterial killing without inducing septic symptoms as obtained by injection of free bromelain and ciprofloxacin. This shows the advantage of simultaneous release from liposomes of bromelain and ciprofloxacin inside a biofilm.

1. Introduction

Dispersal of infectious biofilms is frequently considered as a new approach for treating recalcitrant bacterial infections [1]. A major problem associated with dispersal approaches is the sudden presence of high concentrations of bacteria dispersed from a biofilm in the blood circulation [2,3], at a rate that is higher than the immune system can deal with [2]. In order to prevent septic complications resulting from the dispersal of infectious biofilm, it is imperative that that dispersed bacteria are killed immediately after their dispersal [4]. Bromelain is a pineapple extract composed of a variety of proteolytic enzymes, phosphatases, glucosidases, peroxidases, cellulases and glycoproteins [5–7] and has recently been demonstrated [8] to enhance antibiotic efficacy through degradation of biofilm matrices yielding dispersal of biofilm bacteria. Clinically however, effective, simultaneous delivery of bromelain into an infectious biofilm together with an antibiotic is extremely difficult, due to the short half-life time of bromelain in blood [9,10].

Nanocarriers like nano-capsules [11,12], micelles [13,14] and liposomes [15,16] are frequently considered nowadays for encapsulation and delivery of enzymes and antibiotics. Release of therapeutic cargo from nanocarriers from the blood circulation must preferentially be confined to a target site, such as inside an infectious biofilm or tumor. Controlled cargo release can be achieved through “internal” stimuli such as pH, hypoxia or temperature or alternatively through “external” stimuli like light irradiation or ultrasound application [17]. Unlike micelles that possess a hydrophobic core, liposomes can be loaded with a hydrophobic (in-membrane) and hydrophilic (in-core) cargo. Moreover, several liposome-based medicines have been approved by the FDA [18]. However, confining cargo release from liposomes to a target site requires conjugation of stimuli-responsive functionalities with membrane lipids that may disrupt the physico-chemical balance in the lipid

* Corresponding authors.
E-mail addresses: h.c.van.der.mei@umcg.nl (H.C. van der Mei), h.j.busscher@umcg.nl (H.J. Busscher), shilinqi@nankai.edu.cn (L. Shi).

https://doi.org/10.1016/j.jconrel.2022.10.049
Received 29 July 2022; Received in revised form 7 October 2022; Accepted 25 October 2022
Available online 1 November 2022

membrane of liposomes [17,19]. Recently, we synthesized a lipid named DCPA (2-(4-((1,5-bis(octadecenoyl)1,5-dioxopentan-2-yl)carbamoyl) pyridin-1-ium-1-yl)acetate) that complexes with water through hydrogen bonding (DCPA-H_2O) [20]. Water molecules in DCPA-H_2O liposomes provide a stealth functionality that allows long-time blood circulation, while becoming protonated below pH 6.8 allowing fast self-targeting to infectious biofilms after tail-vein injection in mice.

Based on the hypothesis that simultaneous release of a dispersant and an antibiotic inside an infectious biofilm can prevent septic symptoms, the aim of this paper was to investigate whether self-targeting DCPA-H_2O liposomes can be dual-loaded with a dispersant and an antibiotic for simultaneous release inside an infectious biofilm. To this end, for the first time, we explored the possibility of in-membrane and in-core, dual-loading of self-targeting DCPA-H_2O liposomal nanocarriers for the controlled and simultaneous release of bromelain and a clinically applied, broad-spectrum antibiotic (ciprofloxacin) inside a biofilm. DCPA-H_2O liposomes were core-loaded with bromelain. Ciprofloxacin was made amphiphilic by PEGylation so that PEGylated ciprofloxacin could become integrated as a membrane component in the lipid membrane of the DCPA-H_2O liposomes (see Scheme 1a). Controlled release was hypothesized to be proton-mediated in the acidic environment of an infectious biofilm, purposely disrupting the physico-chemical balance in the lipid membrane of the liposomes to yield their burst and therewith cargo release (see Scheme 1b).

2. Materials and methods

2.1. Materials and reagents

1,4-dioxane, dimethyl sulfoxide (DMSO), dichloromethane (DCM), petroleum ether (PE), ethyl acetate (EA), acetonitrile (MeCN), tetrahydrofuran (THF), *N*,*N*-dimethylformamide (DMF), hydrochloric acid (HCl), sodium hydroxide (NaOH), sodium chloride (NaCl), and anhydrous sodium sulfate (Na_2SO_4) were purchased from Tianjin Bohua Chemical Reagent Co. Ltd. (Tianjin, China). Bromelain, tryptone soy agar (TSB), and ciprofloxacin were purchased from Dalian Meilun Biotech Co., Ltd. (Dalian, China). The PEG_{2K}-OH, $CDCl_3$ and DMSO-d_6 were purchased from Beijing Innochem Science & Technology Co, Ltd. (Peking, China). Trifluoroacetic acid (TFA), 4-dimethylaminopyridine (DMAP), (1H-Benzotriazole-1-yl)-1,1,3,3-tetramethyl-uronium hexafluorophosphate (HBTU), rhodamine B and glutaric dialdehyde were purchased from Heowns Biochem Technologies LLC. (Tianjin, China). Concanavalin A-tetramethylrhodamine was purchased from Xi'an Ruixi Biotechnology Co., Ltd. (Xi'an, China). Gelatin was purchased from Shanghai Aladdin Biochemical Technology Co., Ltd. (Shanghai, China).

2.2. Bacterial strain, culturing and harvesting

Green-fluorescent *Staphylococcus aureus* ATCC12600^{GFP} was cultured, as described before [21]. Briefly, *S. aureus* ATCC12600^{GFP} was cultured from a frozen stock onto tryptone soy agar (TSB) plates supplemented with 10 μg/mL tetracycline at 37 °C, For experiments, one colony was transferred to inoculate 10 mL of TSB, also supplemented with 10 μg/mL tetracycline for *S. aureus* ATCC12600^{GFP} at 37 °C for 24

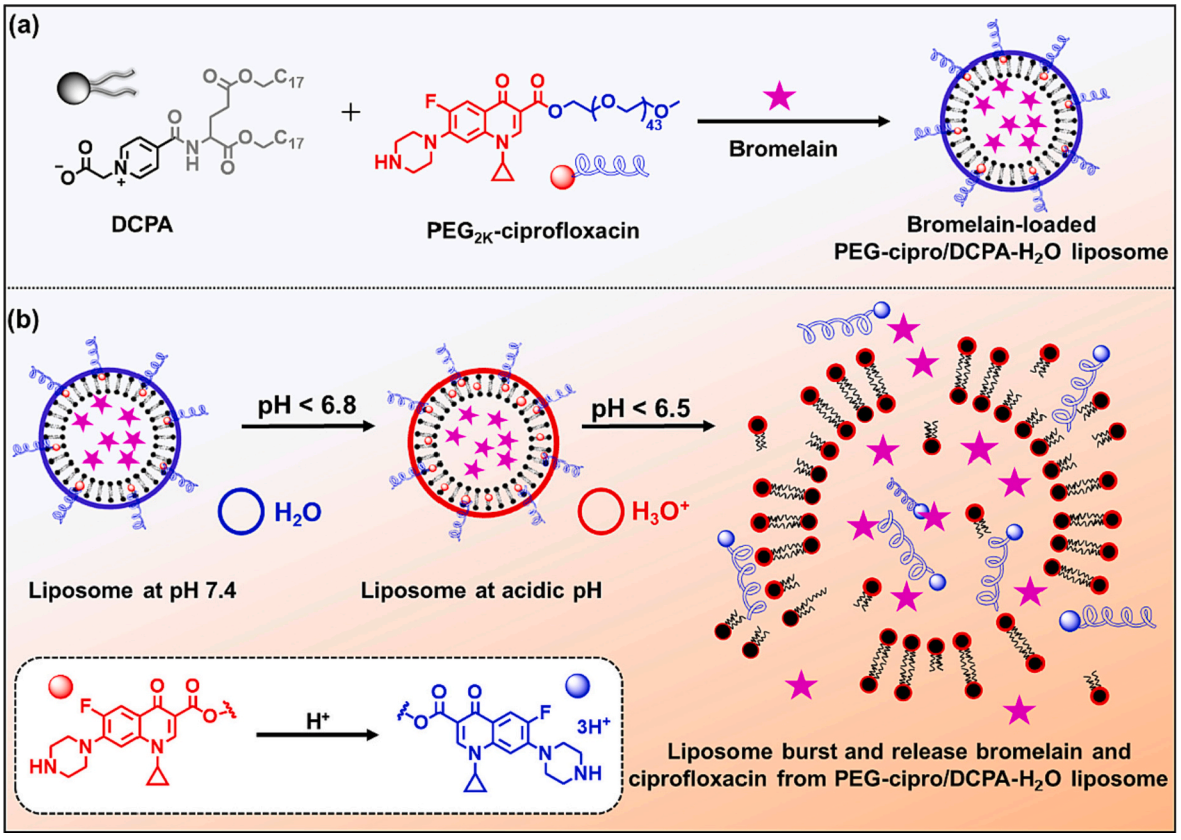

Scheme 1. Preparation of bromelain-loaded PEG-cipro/DCPA-H_2O liposomes with proton-mediated controlled release of bromelain and PEGylated ciprofloxacin. (a) DCPA and PEGylated ciprofloxacin were allowed to self-assemble in the presence of bromelain to yield bromelain-loaded liposomes with PEGylated ciprofloxacin incorporated in the lipid membrane of the liposomes. (b) In the acidic environment of an infectious biofilm, protonation of water and PEGylated ciprofloxacin causes a hydrophilicity and charge disbalance in the lipid membrane of the liposomes, yielding burst of the liposomes and therewith release of core-loaded bromelain and PEGylated ciprofloxacin as a membrane component.

h. This pre-culture was diluted 1:20 in 100 mL TSB and grown statically for 12 h at 37 °C. Cultures were harvested by centrifugation for 5 min at 5000*g* at 4 °C, washed three times with fresh phosphate buffered saline (PBS, 1.8 mM KH_2PO_4, 10 mM Na_2HPO_4, 137 mM NaCl and 2.7 mM KCl), sonicated for 3 × 10 s (Vibra cell model 375, Sonics and Material Inc., Danbury, CT) while cooling in an ice/water bath to break bacterial aggregates. Finally, suspensions were diluted in PBS to concentrations required in the respective experiments, as determined OD_{600} using Microdrop.

2.3. Animals

Seven to eight weeks-old, healthy female BALB/c nude mice were purchased from SLAC Laboratory Animal Co., Ltd. (Shanghai, China). Upon purchase, the average weight of the mice amounted 16.4 ± 0.1 g. Male Spraque Dawley rats were purchased from Vital River Laboratories (Beijing, China). Rats weighed 287 ± 6 g upon purchase and were randomly divided into four groups of three animals. All animals were housed in the on-site animal facility of Nankai University and experimental procedures were approved by the Institutional Animal Care and User Committee of Nankai University, Tianjin, China (approval number: 2021-SYDMLL-000454).

2.4. Lipid synthesis

DCPA was prepared as previously described [20] and the chemical structure was identified by ^{1}H NMR. PEG_{2K}-ciprofloxacin was prepared according to the following procedure. Briefly, ciprofloxacin (1.0 g, 3 mmol) was dissolved in 20 mL dioxane:water (1:1). Then, 4.5 mL 1.0 M NaOH and di-tertbutylcarbonate (1.0 g, 4.5 mmol) was added and the mixture was stirred at ambient temperature for 2 h. Thin layer chromatography was applied to monitor whether the reaction was completed. Acetone (20 mL) was added to precipitate the ciprofloxacin-Boc and the solid product was filtered and washed with acetone. The solid was dried under vacuum to obtain 1.21 g ciprofloxacin-Boc as white powder (93% yield).

PEG_{2K}-OH (2.78 g, 1.38 mmol) was added to a mixture of ciprofloxacin-Boc (200 mg, 0.46 mmol), HBTU (439.9 mg, 1.16 mmol) and DMAP (10.91 mg, 0.09 mmol) in dry DCM (50 mL) under N_2 protection. After stirring at ambient temperature for 10 h, the solution was washed twice with saturated NaCl solution (50 mL) and the resulting organic layer was collected, dried with anhydrous Na_2SO_4 and Na_2SO_4 was removed by filtration. Next, the solution was distilled under vacuum to remove DCM and obtain crude PEG_{2K}-ciprofloxacin-Boc. PEG_{2K}-ciprofloxacin-Boc was purified by column chromatography with silica gel and a gradient of DCM:MeOH (50:1) yielding 860.7 mg white powder (81% yield).

Removal of the Boc-protector from PEG_{2K}-ciprofloxacin-Boc (500 mg, 0.21 mmol) was performed by dropwise addition of 5 mL TFA in 5 mL DCM solution under N_2 protection at 0 °C to obtain PEG_{2K}-ciprofloxacin trifluoroacetate. The mixture was stirred for 30 min at room temperature. Rotary evaporation under reduced pressure yielded a white yellow solid film and 5 mL DMSO was added to dissolve the solid film. Subsequently, the solution was transferred to a dialysis bag (molecular weight cutoff (MWCO) 1 kDa) and dialyzed against deionized water (pH 7.4, adjusting with 1 M NaOH) for 24 h to remove DMSO and trifluoroacetate. Finally, PEG_{2K}-ciprofloxacin, as light-yellow oil (418 mg, yield 86%), was obtained by lyophilization.

2.5. Self-assembly of liposomes, bromelain and additional ciprofloxacin loading

For the synthesis of bromelain-loaded PEG-cipro/DCPA-H_2O liposomes (B-PEG-cipro/DCPA-H_2O), DCPA (10 mg) and PEG_{2K}-ciprofloxacin (1 mg) were dissolved in 1 mL THF. This facilitated self-assembly of liposomes with amphiphilic PEGylated ciprofloxacin as an in-membrane component. For in-core loading of bromelain, this solution was injected in 10 mg bromelain dissolved in 10 mL deionized water under vigorous stirring with a magnetic bar (600 rpm) in a water bath kept at 50 °C. After 5 min, the solution was transferred to a dialysis bag (MWCO 50 kDa) and dialyzed against deionized water for 24 h. Deionized water was refreshed 3 times per day to remove organic solvent. For additional, in-membrane loading of ciprofloxacin, bromelain-loaded B/C-PEG-cipro/DCPA-H_2O liposomes, DCPA (10 mg), ciprofloxacin (1 mg) and PEG_{2K}-ciprofloxacin (1 mg) were dissolved in 1 mL organic solvent (THF: DMSO = 4:1) at 50 °C, similar as described for B-PEG-cipro/DCPA-H_2O. After dialysis, the resulting liposome suspension was filtered using a syringe with 0.45 μm filtration membrane (Merck, America) in order to remove liposomes >0.45 μm. Finally, the liposome suspension was concentrated by low-speed ultrafiltration (15 min, ×1247 g) using a filter with a nominal molecular weight limit of 10 kDa (Merck Millipore, Massachusetts, USA). Liposome concentrations were determined by measuring the weight of liposome powder obtained by lyophilizing 200 μL of a liposome suspension. Before each experiment, the liposome suspension was filter-sterilized (MILLEX®GP 0.22 μm).

2.6. Bromelain and ciprofloxacin loading efficiencies

For the measurement of Rh-bromelain and in-membrane ciprofloxacin loading efficiencies, 1 mL of a liposome suspension in PBS (5.0 mg/mL, pH 7.4) was transferred into a dialysis bag (MWCO 10 kDa) and subsequently immersed in 20 mL of PBS (pH 5.0) at 37 °C. After gently shaking 24 h, an aliquot (1 mL) of the dialysis solution was taken and fluorescence emission spectroscopy (F-700, Hitachi, Tokyo, Japan) was applied to measure the bromelain concentration. For calibration, red-fluorescence intensity was measured between 560 and 650 nm (excitation wavelength 545 nm) as a function of the concentration of Rh-bromelain in PBS (pH 5.0). UV–vis absorption spectroscopy (Shimadzu, Shanghai, China) was applied to determine the in-membrane ciprofloxacin loading efficiency. To this end, a calibration curve was prepared of the UV–vis absorption at 277 nm as a function of ciprofloxacin concentration. Loading efficiencies were subsequently calculated according to

$$LE\% \frac{weight\ of\ loaded\ cargo}{total\ weight\ of\ lipid\ and\ loaded\ cargo} \times 100\% \quad (1)$$

2.7. Release of bromelain and ciprofloxacin

Bromelain and additional, in-membrane ciprofloxacin release was essentially measured as above described using a dialysis bag, but as a function of time up to 24 h and at pH 7.4, 6.5 and 5.0, using fluorescence emission spectroscopy and UV–vis absorption. Possible release of PEG_{2K}-ciprofloxacin as a liposome membrane component during dialysis was done by comparing the ^{1}H NMR spectra of freeze-dried PEG-cipro/DCPA-H_2O liposomes before and after dialysis (see above). Dialysis solutions were freeze-dried, after which freeze-dried powders were dissolved in $CDCl_3$ for ^{1}H NMR spectroscopy. The ratio of peak area at 4.12 ppm of DCPA and PEGylated ciprofloxacin was used to determine the amount of PEG_{2K}-ciprofloxacin released as a membrane component during dialysis.

2.8. Characterization of liposomes

Hydrodynamic diameters and polymer dispersity indices (PDIs) of all liposomes (0.05 mg/mL) dispersed in PBS were measured by dynamic light scattering using a Malvern Zetasizer Nano-ZS90 apparatus (25 °C). Zeta potentials of liposomes (0.05 mg/mL) dispersed in PBS with different pH were also measured using a Zetasizer (Malvern Nano-ZS90). Measurements were carried out in triplicate with separately prepared liposome suspensions.

Transmission Electron Microscopic (TEM) samples were prepared on

200 mesh carbon film supported copper grids. One drop of a liposome solution (5 μL, 0.1 mg/mL) was placed on the grid and allowed to sediment for 60 s. Filter paper was then used to remove the residual solution. The copper grids were treated with phosphotungstic acid for 30 s and dried in vacuum at 37 °C for 48 h. The resulting samples were imaged using Talos TM F200C TEM at 200 kV.

2.9. Dispersal of bacterial biofilm in vitro

1 mL *S. aureus* ATCC 12600^{GFP} in suspension (10^8 bacteria/mL) in PBS was added to a confocal culture dish at 37 °C for 1 h to allow bacteria to sediment and adhere to the well surface. Subsequently, the bacterial suspension was removed, the well was washed 2 times with 1 mL of PBS to remove non-adhering bacteria and 1 mL TSB medium was added to the dishes. Culture dishes were incubated for 48 h at 37 °C and medium was refreshed after 24 h. After 48 h, biofilms were rinsed three times with PBS to remove non-adhering bacteria and exposed to PBS, ciprofloxacin at its minimal bactericidal concentration (10 μg/mL, see Table S1) in PBS, bromelain (10 μg/mL) in PBS, suspensions of B-PEG-cipro/DCPA-H_2O (loaded bromelain 10 μg/mL) or B/C-PEG-cipro/DCPA-H_2O (loaded 10 μg/mL ciprofloxacin and10 μg/mL bromelain) for 1 h. After exposure, the liquid was removed and the biofilm was washed twice with fresh PBS. Subsequently, these biofilms were stained with red-fluorescent concanavalin A for 30 min in the dark to visualize biofilm matrix, the biofilms were washed two times with fresh PBS before imaging using a laser scanning confocal microscopy (CLSM; TCS SP8, Leica, Wetzlar, Germany). An argon ion laser (488 nm) and a green He/Ne laser (561 nm) were used to excite the GFP and rhodamine labeled concanavalin A, respectively. Fluorescence was collected at 500–535 nm (GFP) and 580–610 nm (rhodamine). All data were acquired and analyzed using Leica software, version 2.0 to yield biofilm thickness prior to and after exposure to liposomes as well as relative biomass.

For scanning electron microscopic (SEM) analysis, biofilms were cultured on glass slides in 24-well plates, as described above. After exposure to PBS or bromelain (10 μg/mL), ciprofloxacin (10 μg/mL) or B/C-PEG-cipro/DCPA-H_2O (loaded 10 μg/mL ciprofloxacin and 10 μg/mL bromelain) for 1 h, the biofilms were washed twice carefully with PBS and fixed with 2.5% glutaraldehyde for 2 h at 4 °C. After fixation, samples were dehydrated with a series of graded ethanol solutions. Finally, samples were gold-coated by sputtering and imaged using Quanta 200 SEM (FEI, Hillsboro, OR, USA).

2.10. Self-targeting and accumulation of liposomes in an infectious biofilm underneath an abdominal imaging window in mice

Self-targeting of liposomes to an infectious biofilm was studied as done before [20]. Briefly, mice were anesthetized by intraperitoneal injection of 0.3 wt% pentobarbital sodium (40 mg/kg). Then, the right flanks of the mice were disinfected with 75% (*v*/v) ethanol and a lateral incision was made through the skin and the abdominal wall and a suture was sewed along the edge of the wound. A sterilized abdominal imaging window, consisting of a circular glass coverslip (12 mm diameter; Thermo Scientific, Waltham, Massachusetts, USA) in a titanium frame, was placed glass side up in the incision. The skin and the abdominal wall were placed in a slot, prepared in the side of the titanium frame. Finally, sutures were tightened to secure the window-frame firmly in the animal. After the surgery, the mice were kept at 37 °C until fully recovered. After full recovery, usually requiring 2 days, mice were anesthetized and injected with 200 μL green fluorescent *S. aureus* ATCC12600^{GFP} (10^9 bacteria/mL) underneath the abdominal imaging window to grow a biofilm. After 48 h of biofilm growth, mice were tail-vein injected with (100 μL) Rh-bromelain (0.25 mg/mL) and Rh-bromelain loaded liposome suspensions containing an equivalent Rh-bromelain concentration. After injection, when the images were taken, mice were anesthetized and intravital images were taken in a Caliper IVIS Lumina II (NightOWLIILB983, Berthold Technologies, Germany) as a function of time up to 24 h. All images were acquired with the following parameters: exposure time 0.5 s, emission wavelength 520 nm, excitation wavelength 480 nm. In vivo self-targeting of each group was monitored in three mice. The acquired images were analyzed with Living Image 4.5.1 software (IndiGO, version 2.0.5.0).

2.11. In vivo eradication of a staphylococcal infection underneath an abdominal imaging window in mice

After 48 h of biofilm growth underneath the window, treatment consisted of tail-vein injection every other day starting on day 0 with 100 μL of PBS, bromelain (200 μg/mL) in PBS, bromelain and ciprofloxacin in PBS (each 200 μg/mL), 100 μL B/C-PEG-cipro/DCPA-H_2O liposomes (200 μg/mL ciprofloxacin and bromelain). Injection was carried out at day 0, 2, and 4, and intravital images were acquired each on day 0, 1, 3 and 5 by two-photon laser scanning confocal microscope (Leica, TCS SP8 STED 3×, Germany). After sacrifice at day 5, 1 g of tissue surrounding the wound was excised, and homogenized in PBS. The homogenate was serially diluted and plated on TSB agar plates. After incubation for 24 h at 37 °C, number of colonies forming units (CFUs) were enumerated. During the course of the experiment, activity of the mice was monitored and body weight and temperature measured.

2.12. Statistical analysis

All data shown represent means ± standard deviations (SD) and were examined for statistically significant differences using a two-tailed Student's *t*-test (GraphPad Prism 8).

3. Results and discussion

3.1. Lipid synthesis

Liposomes were prepared by self-assembly of DCPA (2-(4-((1,5-bis (octadecenoyl)1,5-dioxopentan-2-yl) carbamoyl) pyridin-1-ium-1-yl) acetate) and PEG_{2K}-ciprofloxacin. DCPA was synthesized as described before [20] and summarized for completeness in Scheme S1a. The chemical structure of DCPA was confirmed using ^{1}H NMR (Fig. S1).

Amphiphilic PEG_{2K}-ciprofloxacin was prepared as described in Scheme S1b. ^{1}H NMR confirmed the chemical structure of intermediate reaction compounds (Fig. S2 and Fig. S3) as well as of PEG_{2K}-ciprofloxacin (Fig. S4).

3.2. Self-assembly of liposomes and their characterization

Self-assembly of DCPA and amphiphilic PEG_{2K}-ciprofloxacin into liposomes is new and required optimization of the concentration ratio of PEG_{2K}-ciprofloxacin over DCPA. First, DCPA and PEG_{2K}-ciprofloxacin were mixed in different weight ratios in 1 mL tetrahydrofuran (THF) in absence of bromelain. Then, the solvent was injected into 10 mL bromelain solution in deionized water, yielding in-core loading of bromelain in PEG-cipro/DCPA-H_2O liposomes. When the ratio of PEGylated ciprofloxacin over DCPA exceeded 0.1, the hydrodynamic diameter and polydispersity indices of the liposomes formed increased rapidly (Fig. 1a) to values considered too high for the prevention of reticulo-endothelial rejection and biofilm penetration [22]. Moreover, at higher ratios liposomes became unstable during storage (Fig. 1b).

Therefore, in the remainder of this work, liposomes were formed by mixing 10 mg DCPA and 1 mg PEG_{2K}-ciprofloxacin in 1 mL THF. 10 mL bromelain in deionized water (1 mg/mL) was added to the mixture to yield bromelain-loaded PEG-cipro/DCPA-H_2O liposomes. To determine the loading efficiency, bromelain was Rhodamine B labeled (see Fig. S5a for ^{1}H NMR spectra). Fluorescence emission spectroscopy was subsequently applied (see Fig. S5b for spectra), after preparation of a calibration curve (see Fig. S5c) to yield the loading efficiency of bromelain, amounting 12 ± 2%. Since amphiphilic PEG_{2K}-ciprofloxacin is only

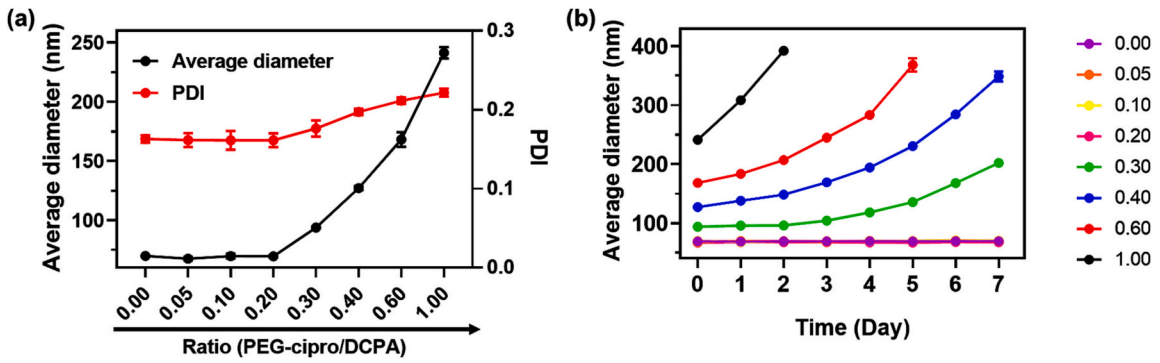

Fig. 1. Diameter and storage stability of bromelain-loaded PEG-cipro/DCPA-H_2O liposomes containing different weight ratios of amphiphilic PEG_{2K}-ciprofloxacin to DCPA. (a) Average diameter and polydispersity indices (PDI) of liposomes as a function of the weight ratio of PEG_{2K}-ciprofloxacin (PEG-cipro) to DCPA suspended in deionized water and measured using dynamic light scattering. (b) Average diameters of liposomes containing different weight ratios of PEG_{2K}-ciprofloxacin to DCPA as a function of time during suspension (50 μg/mL) in phosphate buffered saline. Note that data for weight ratios of 0.00, 0.05, 0.10 and 0.20 are overlapping. (For interpretation of the references to colour in this figure legend, the reader is referred to the web version of this article).

weakly antibacterial as compared with hydrophobic ciprofloxacin (Table S1), the above described self-assembly procedure was also carried out in presence of ciprofloxacin (1 mg) to facilitate in-membrane loading of ciprofloxacin in addition to in-membrane PEG_{2K}-ciprofloxacin in bromelain-loaded PEG-cipro/DCPA-H_2O liposomes. Liposomes could be additionally in-membrane loaded with ciprofloxacin with a loading efficiency of 10 ± 1%, as determined using UV–vis absorption spectroscopy (see Fig. S6). Note that during dialysis, a minor loss (6.8%) of PEG_{2K}-ciprofloxacin as a membrane component occurred (Fig. S7).

Average diameters of bromelain-loaded DCPA-H_2O, bromelain-loaded PEG-cipro/ DCPA-H_2O and bromelain-loaded PEG-cipro/DCPA-H_2O with additional ciprofloxacin-loading were all hoovering between 65 and 69 nm, with a PDI of around 0.2 (Fig. 2a). All liposomes demonstrated a spherical morphology (Fig. 2b). The pH-responsiveness of bromelain-loaded DCPA-H_2O, bromelain-loaded PEG-cipro/DCPA-H_2O and bromelain-loaded PEG-cipro/DCPA-H_2O with additional ciprofloxacin-loading was virtually identical, with zeta potentials becoming positive for pH values below 7.0 (Fig. 2c). A negative zeta potential at physiological pH is of major importance for allowing long circulation in blood [23,24], while a reversal to a positive zeta potential is pivotal for self-targeting to acidic tumor or infection sites [20,25].

3.3. *In vivo blood circulation times of bromelain-loaded PEG-cipro/DCPA-H_2O liposomes and self-targeting of an abdominal biofilm*

Next, it was evaluated whether blood circulation times of bromelain had indeed benefited from en-capsulation in PEG-cipro/DCPA-H_2O liposomes by measuring bromelain concentrations in the blood of rats after tail-vein injection. Bromelain freely dissolved in blood was cleared from the blood circulation within 6 h, which is considerably faster than when loaded in any of the liposomes involved in this study (Fig. 3a). Accordingly, the half-life time of free bromelain in blood increased from

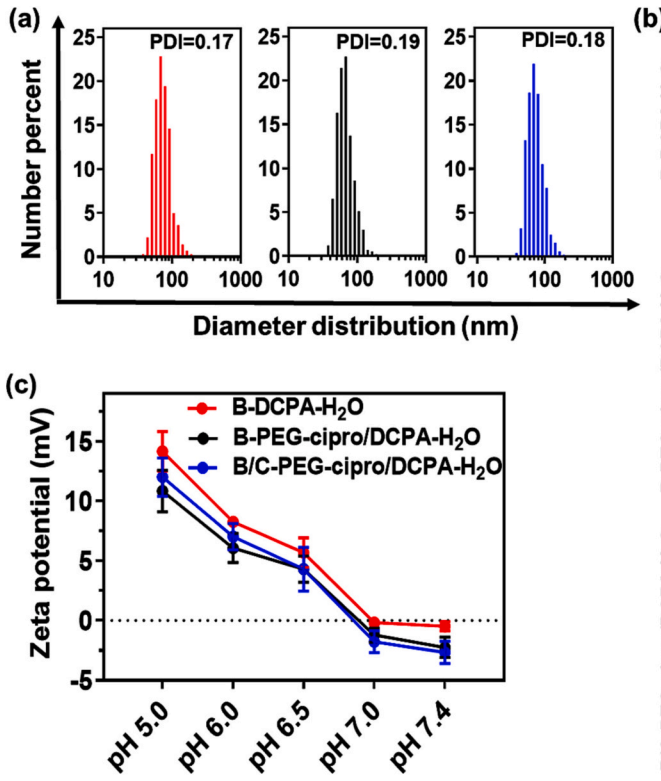

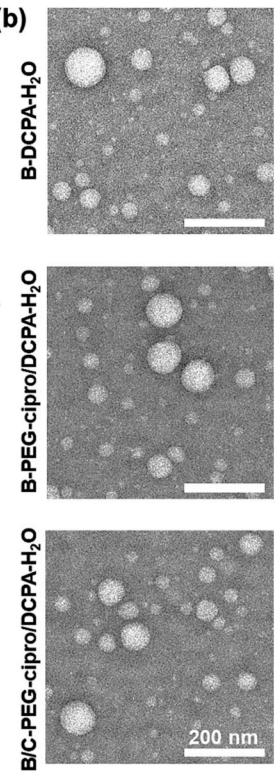

Fig. 2. Diameters, micrographs and zeta potentials of bromelain-loaded DCPA-H_2O (B-DCPA-H_2O), PEG-cipro/DCPA-H_2O (B-PEG-cipro/DCPA-H_2O) and B/C-PEG-cipro/DCPA-H_2O liposomes with additional ciprofloxacin-loading. (a) Diameter distributions and PDI of liposomes suspended in PBS measured using dynamic light scattering. (b) Transmission electron micrographs of liposomes. (c) Zeta potentials of liposomes as a function of pH in a PBS with pH adjusted with HCl or NaOH. Zeta potentials were measured immediately (within 2 min) after suspending in PBS with a specific pH. All error bars denote standard deviations over triplicate experiments with separately prepared batches of liposomes. (For interpretation of the references to colour in this figure legend, the reader is referred to the web version of this article).

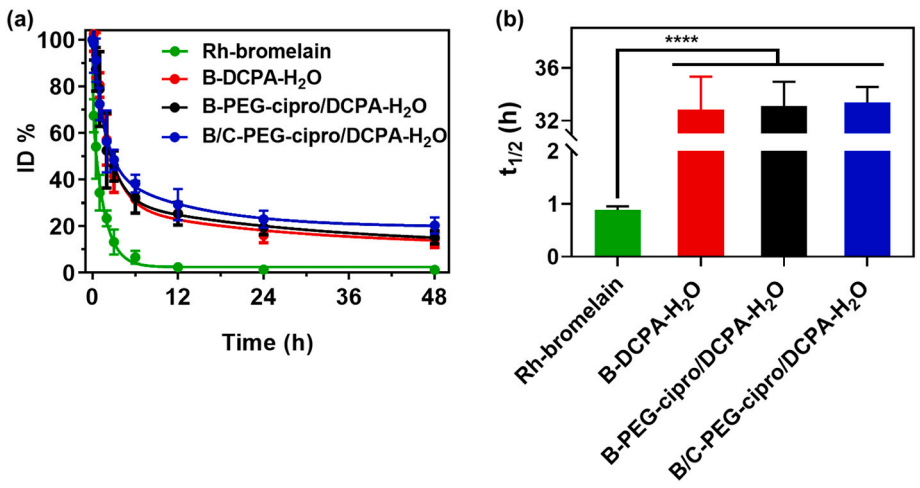

Fig. 3. Blood circulation times of Rhodamine-labeled bromelain in B-DCPA-H_2O, B-PEG-cipro/DCPA-H_2O and B/C-PEG-cipro/DCPA-H_2O liposomes with additional ciprofloxacin-loading after tail-vein injection in rats. (a) Percentage of red-fluorescent Rh-bromelain or Rh-bromelain loaded liposomes as a function of time after tail-vein injection, expressed as a percentage of the injected dose (ID). The injected dose amounted 1.0 mg/kg (0.5 mL at a bromelain concentration of 600 μg/mL. Bromelain and liposome concentrations were measured employing fluorescence emission spectroscopy (see Fig. S8 for calibration curves in rat plasma). (b) Blood circulation half-life times of bromelain, calculated from the data in panel (a). All error bars denote standard deviations over three rats in each group. (For interpretation of the references to colour in this figure legend, the reader is referred to the web version of this article).

around 1 h to between 33 and 35 h upon transport within liposomes (Fig. 3b), which is significantly longer than freely dissolved bromelain in blood or orally administered bromelain in human intestines, that has been described to remain biologically active with a half-life of 6–9 h [9].

Self-targeting to a green-fluorescent staphylococcal biofilm of bromelain and bromelain-loaded liposomes was studied in mice, using an abdominal window model [20] (see Fig. 4a for experimental scheme). The abdominal window uniquely allows for real-time observation of a fluorescent biofilm and its targeting by fluorescent nanocarriers [26–28]. Quantitative analyses of intra-abdominal images of a *S. aureus* biofilm underneath an abdominal window in mice after tail-vein injection of bromelain or liposomes (Fig. 4b), demonstrated minor, short-lived accumulation of Rhodamine-labeled bromelain in the biofilm. However, protected in self-targeting liposomes, bromelain accumulation in biofilms continued to increase up to 6 h (Fig. 4c). Notably, the maximum accumulation of bromelain loaded in self-targeting liposomes was 5 times higher 24 h after tail-vein injection than when injected freely dissolved in PBS (Fig. 4d).

3.4. Proton-mediated, controlled release of bromelain and ciprofloxacin from PEG-cipro/DCPA-H_2O liposomes

At pH 7.4, bromelain and in-membrane ciprofloxacin release was similarly small for all types of liposomes included (Fig. 5a and Fig. 5b, respectively). Both bromelain (Fig. 5a) and ciprofloxacin (Fig. 5b) release remained small at more acidic pH down to at least pH 5.0 when released from bromelain-loaded DCPA-H_2O liposomes. However, when released from PEG-cipro/DCPA-H_2O liposomes, bromelain release increased to almost 100% of the initial loading within 24 h. Concurrent with increasing cargo release, the diameter of PEG-cipro/DCPA-H_2O liposomes increased with decreasing pH (Fig. 5c), ultimately leading to a burst and full disintegration of the liposomes (Fig. 5d). Bromelain-loaded DCPA-H_2O liposomes remained fully intact. This confirms our hypothesis that PEGylated ciprofloxacin in the liposomal membrane acts as a proton-sponge and becomes positively charged at low pH, disrupting the charge balance in the membrane and causing burst of the liposomes (see Scheme 1b). This method of creating a burst of the lipid membrane of liposomes yielded simultaneous release of both in-membrane and in-core cargo. Moreover, this proton-mediated cargo release was faster than can be achieved using both pH-responsive liposomes or pH-responsive micelles that typically possess conjugated pH-responsive functionalities, reacting through slower ring opening (topotecan hydrochloride) [29], triggering of phase transitions (methacryloyl sulfadimethoxines) [30], or lipid breaking switch (orthoester [31], vinyl ester [32], hydrazine [33] and Schiff bases [34].

Circular dichroism (CD) spectra of bromelain in PBS and bromelain released from bromelain-loaded PEG-cipro/DCPA-H_2O liposomes (Fig. 5e), both demonstrated two negative bands at 208 and 222 nm, characteristic for α-helix conformation of bromelain [35]. This demonstrates that loading of and release of bromelain did not affect its secondary structure. Accordingly, the enzymatic ability of bromelain was not affected and its ability to degrade gelatin was similar after loading and release as compared with free bromelain (Fig. S9). This is a unique advantage of maintaining the enzymatic activity of bromelain by liposomal encapsulation that could not be achieved by protection of bromelain through chemical modification, yielding 20 to 200 fold lower degradation of gelatin [10,36] than observed here.

3.5. Dispersal of staphylococcal biofilms by bromelain-loaded PEG-cipro/DCPA-H_2O liposomes

Dispersal of green-fluorescent *S. aureus* biofilms was evaluated by exposing staphylococcal biofilms to PBS, bromelain dissolved in PBS with and without ciprofloxacin and in bromelain-loaded PEG-cipro/DCPA-H_2O liposomes with additional ciprofloxacin-loading. After exposure, biofilms were stained with red-fluorescent concanavalin A in order to visualize the EPS matrix. Confocal laser scanning microscopic (CLSM) images (Fig. S10) demonstrated that prior to exposure (i.e. exposure to PBS), staphylococcal biofilms had a thickness of around 35 μm (Fig. 6a) that was not affected by exposure to ciprofloxacin. Exposure to bromelain with or without ciprofloxacin yielded a decrease in biofilm thickness to around 23 μm. However, bromelain-loaded PEG-cipro/DCPA-H_2O liposomes with additional ciprofloxacin-loading yielded the largest dispersal of staphylococcal biofilm, reducing their thickness to around 12 μm. Interestingly, biofilm exposure to ciprofloxacin in solution did not yield a reduction in the number of staphylococcal CFUs, while the reduction in biofilm thickness upon exposure to bromelain in solution was not accompanied by a reduction in the number of CFUs (Fig. 6b). These observations confirm that bromelain is not a bactericidal compound (see also Table S1), and furthermore illustrate that the biofilm mode of growth protects its inhabitants against antibiotic exposure [37,38]. However, combined exposure to bromelain and ciprofloxacin yielded reductions in both biofilm thickness and the number of CFUs, that were largest when bromelain was core-loaded in PEG-cipro-DCPA-H_2O liposomes with additional in-membrane, ciprofloxacin loading (Fig. 6b). Accordingly, the volumetric density of staphylococci in remaining biofilm was lowest after exposure to B/C-PEG-cipro-DCPA-H_2O liposomes (Fig. 6c), due to the synergy between ciprofloxacin killing of biofilm inhabitants, and matrix degradation and biofilm dispersal achieved by bromelain (compare respective SEM micrographs in Fig. 6d).

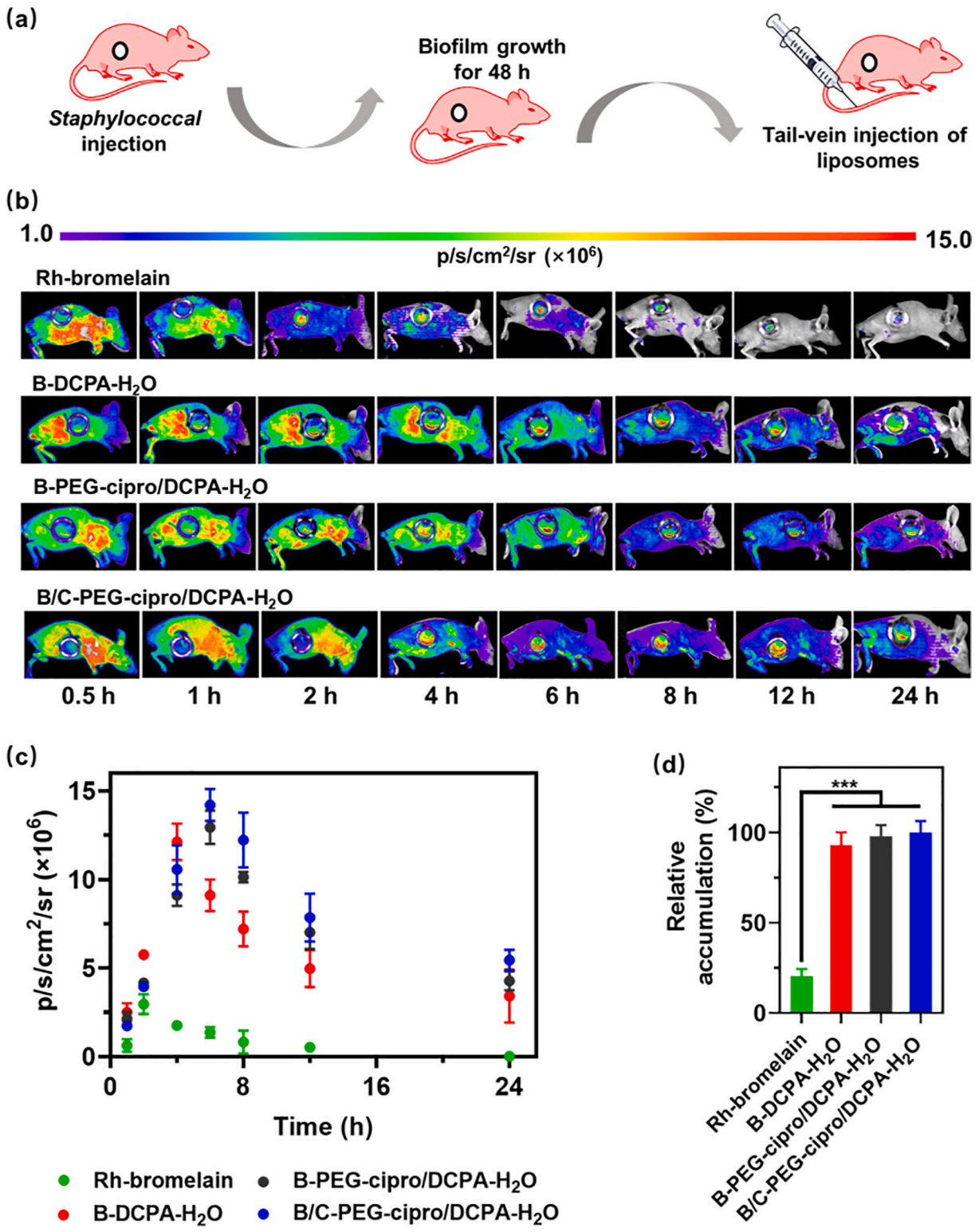

Fig. 4. Self-targeting and accumulation of Rhodamine-labeled bromelain and Rh-bromelain loaded in B-DCPA-H_2O, B-PEG-cipro/DCPA-H_2O and B/C-PEG-cipro/DCPA-H_2O liposomes with additional ciprofloxacin-loading after tail-vein injection in mice. (a) Schematics of intravital imaging of tail-vein injected bromelain and bromelain-loaded liposomes towards a *S. aureus* ATCC12600^{GFP} biofilm underneath an abdominal imaging window. (b) Fluorescence images taken at different times after tail-vein injection of bromelain or bromelain-loaded liposomes. Fluorescence represents Rhodamine-labeled bromelain on a pseudo-colour scale reflecting the fluorescence intensity. (c) Self-targeting of bromelain and bromelain loaded liposomes into infectious biofilm as a function of time after tail-vein injection of liposomes, expressed as total number of photons per second per square centimeter (p/s/cm^2/sr). (d) Percentage accumulation bromelain in infectious biofilms, 24 h after tail-vein injection, expressed with respect to maximum accumulation of B/C-PEG-cipro/DCPA-H_2O liposomes (panel c). All error bars denote SD over three mice in each group. Significance levels (Students' test) for the comparisons are indicated by asterisks: ***$P < 0.001$. (For interpretation of the references to colour in this figure legend, the reader is referred to the web version of this article).

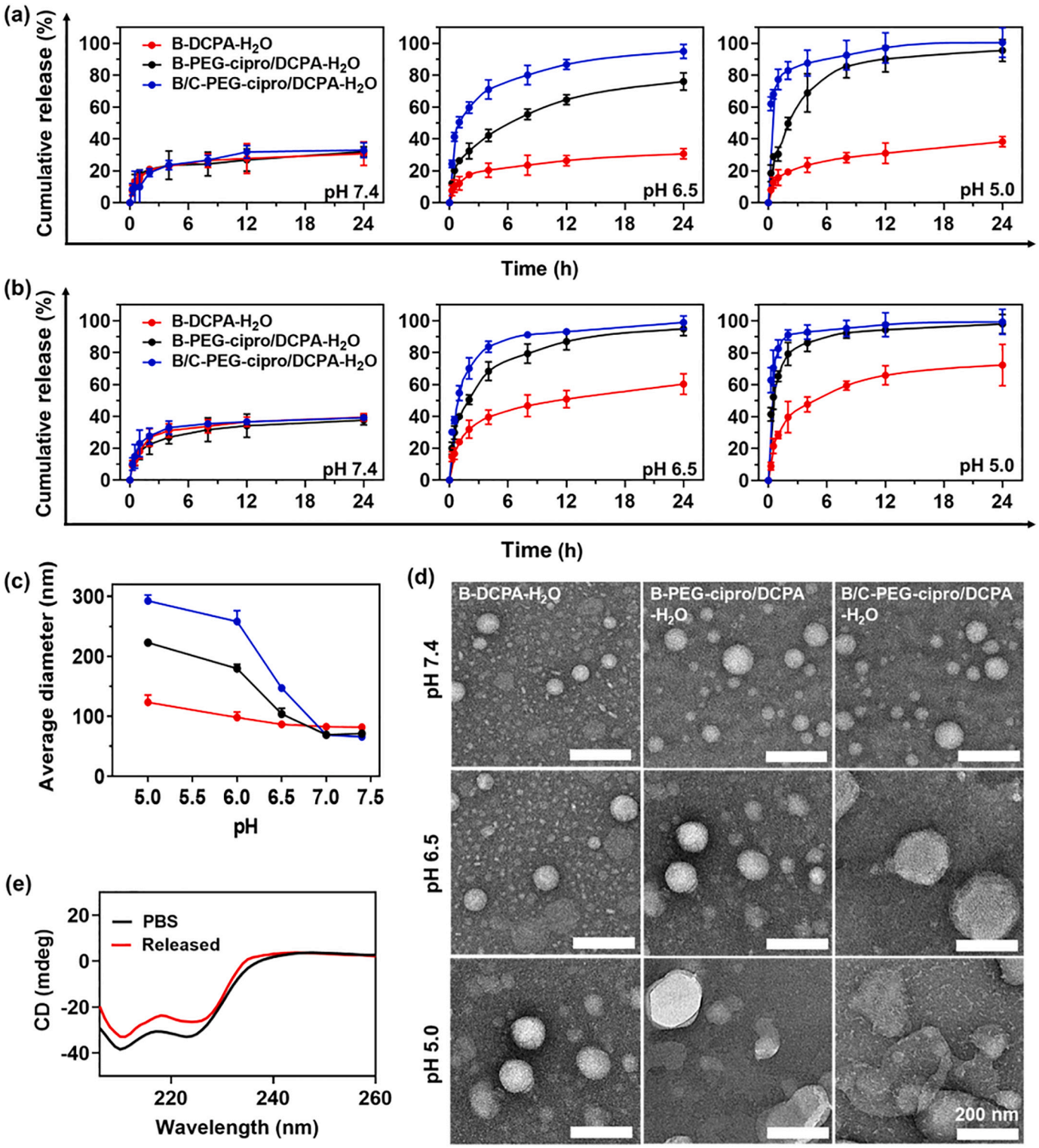

Fig. 5. Controlled release of bromelain and in-membrane ciprofloxacin from B-DCPA-H_2O, B-PEG-cipro/DCPA-H_2O and B/C-PEG-cipro/DCPA-H_2O liposomes with additional ciprofloxacin-loading. (a) Percentage cumulative bromelain release as a function of time at 37 °C from different liposomes, suspended (5 mg/mL) in PBS, with pH adjusted through addition of HCl or NaOH. Release of bromelain was measured using fluorescence emission spectroscopy (see Fig. S5c for a calibration curve) and expressed relative to the total amount of core-loaded bromelain. Error bars denote the standard deviations over triplicate experiments with separately prepared batches of liposomes. (b) Same as panel a, now for ciprofloxacin release from liposome using UV–vis absorption spectroscopy (see Fig. S6b for a calibration curve). (c) Average diameter of bromelain-loaded liposomes obtained using dynamic light scattering after 30 min exposure to PBS at different pH. Error bars denote the standard deviations over triplicate experiments with separately prepared batches of liposomes. (d) Same as panel c, now presenting transmission electron micrographs. (e) CD spectra of bromelain dissolved in PBS and bromelain released from bromelain-loaded liposomes in PBS. (For interpretation of the references to colour in this figure legend, the reader is referred to the web version of this article).

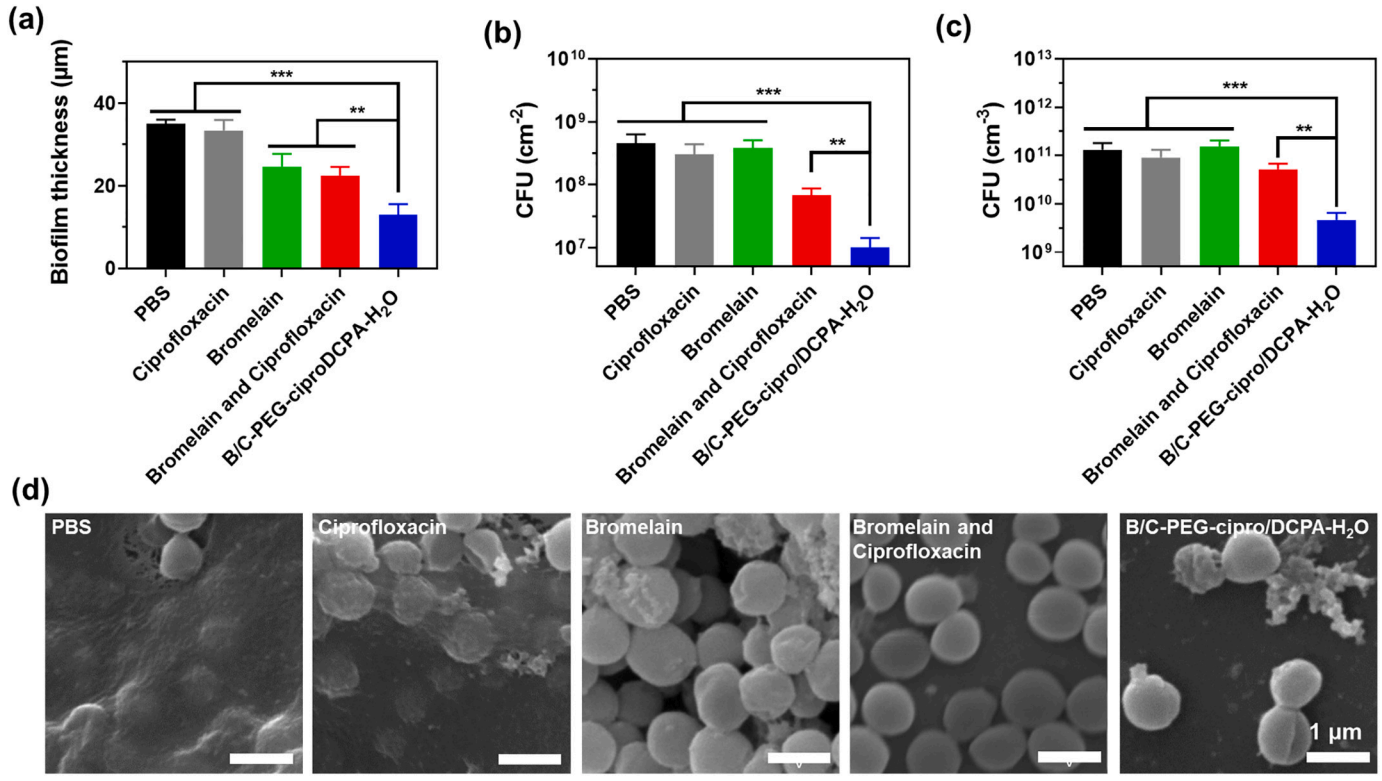

Fig. 6. Dispersal and killing of 2-days-old *S. aureus* ATCC12600^{GFP} biofilms upon 1 h exposure to PBS, ciprofloxacin (10 μg/mL), bromelain (10 μg/mL), bromelain and ciprofloxacin (10 μg/mL of each) or suspensions of bromelain-loaded PEG-cipro/DCPA-H_2O with additional ciprofloxacin-loading (10 μg/mL ciprofloxacin and 10 μg/mL bromelain). (a) Thickness of staphylococcal biofilms derived from CLSM images (Fig. S10). (b) Number of CFUs per unit area retrieved from staphylococcal biofilms. (c) Volumetric density of staphylococci in biofilms left after exposure. (d) SEM micrographs of staphylococci left after exposure. All error bars denote standard deviations over triplicate measurements with separately prepared liposome suspensions and bacteria. Asterisks indicate statistical significance at ** $p < 0.01$,and *** $p < 0.001$.

3.6. In vivo eradication of an abdominal biofilm by bromelain-loaded PEG-cipro/DCPA-H_2O liposomes

In vivo advantages of B/C-PEG-cipro/DCPA-H_2O liposomes for the eradication of infectious biofilms were explored using intra-vital imaging of an abdominal biofilm in living mice (see scheme in Fig. 7a). From the on-set of infection, mice were examined for clinical signs of infection and sepsis, including reduced activity or body weight and low temperature [39]. Mice became inactive immediately after initiating infection with green-fluorescent *S. aureus* and tail-vein injection of PBS, while their weight (Fig. 7b) and body temperature (Fig. 7c) started to decrease as compared with uninfected mice. Also after tail-vein injection of bromelain-only inactivity and weight loss were observed (Fig. 7b). Temperature drop was more severe after injection of bromelain than in case of PBS injection (Fig. 7c), indicative of sepsis arising from the bromelain-induced dispersal of staphylococci into the blood circulation. Septic symptoms. i.e. inactivity, weight loss and decreased temperature could be prevented by injection of bromelain and ciprofloxacin combined in solution or in B/C-PEG-cipro/DCPA-H_2O liposomes. However, as a result of the proton-mediated burst of the liposomes inside the biofilm yielding simultaneous release of bromelain and ciprofloxacin in the close vicinity of the bacteria to be dispersed, septic symptoms were most effectively prevented upon injection of B/C-PEG-cipro/DCPA-H_2O liposomes. This confirms our hypothesis that simultaneous release inside biofilms is required for effective prevention of sepsis after dispersal, although it must be noted that septic symptoms in humans are different from septic symptoms in rodents. Most notably low temperature (hypoxia) is a symptom of sepsis in rodents, while high fever with occasional shivering is a septic symptom in humans [40].

Whereas arguably clinical signs of infection and sepsis may be the real proof of the pudding, more detailed, microbiological analyses of the infecting biofilm itself were also carried out. Fig. 8a presents intra-vital images of the abdominal biofilm at different points in time after initiating treatment from which biofilm thickness could be derived. Biofilm thickness decreased as a function of time after initiating treatment with bromelain combined with ciprofloxacin or B/C-PEG-cipro/DCPA-H_2O liposomes. However, treatment with B/C-PEG-cipro/DCPA-H_2O liposomes yielded significantly better reduction of biofilm thickness than the combination of bromelain and ciprofloxacin in solution (Fig. 8b). The number of CFUs harvested from tissue surrounding the window site, decreased in parallel with the reductions observed in biofilm thickness and were 3 to 4 log units larger in mice treated with B/C-PEG-cipro/DCPA-H_2O liposomes than when treated with PBS (Fig. 8c). Granulocyte counts in blood extracted from mice at sacrifice, were lowest upon treatment with B/C-PEG-cipro/DCPA-H_2O liposomes (Fig. 8d). Collectively, the data in Fig. 8 confirm the course of clinical symptoms presented in Fig. 7.

3.7. In vivo biosafety of bromelain-loaded PEG-cipro/DCPA-H_2O liposomes

Bromelain acts as a proteolytic agent, hydrolyzing peptide and glycosidic bonds in glycoproteins and hydrolyzing complex carbohydrates [41]. This makes bromelain ideal for the degradation of multicomponent biofilm matrices but at the same time creates the need to establish the biosafety of bromelain as a dispersant in vivo. Hence, we performed an extensive blood analysis and histological evaluation of major organ tissue after treatment of a bacterial infection using bromelain-loaded PEG-cipro/DCPA-H_2O liposomes. At sacrifice, no indications were found of any damage to organ tissues (Fig. S11), while

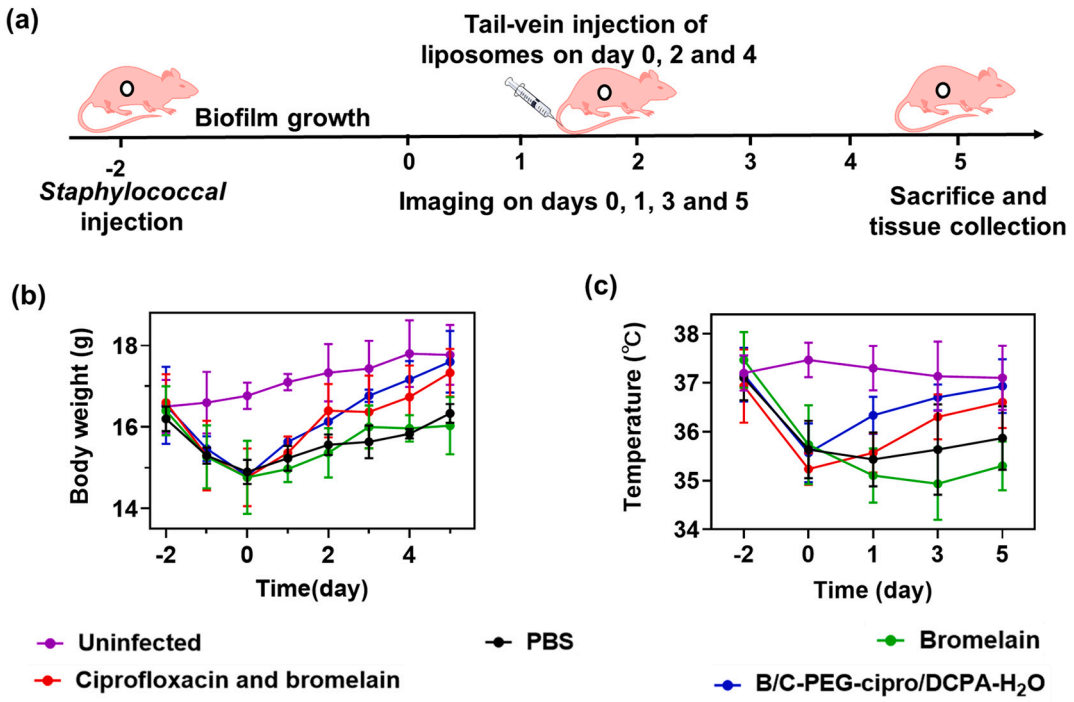

Fig. 7. Clinical signs of infection and sepsis due to dispersal of a *S. aureus* ATCC12600^{GFP} biofilm underneath an abdominal imaging window in mice. (a) Experimental time-line: Growth of an infectious biofilm was initiated by injection of green-fluorescent staphylococci underneath the abdominal window. Two days after initiating infection, treatment was started by tail-vein injection of 0.1 mL PBS, bromelain (200 μg/mL), bromelain and ciprofloxacin (200 μg/mL of each) or suspension of bromelain-loaded PEG-cipro/DCPA-H_2O with additional ciprofloxacin-loading (loaded 200 μg/mL ciprofloxacin and 200 μg/mL bromelain). (b) Body weight of mice in different treatment groups as a function of time after initiating biofilm growth and treatment. Body weight upon entry in the study prior to window implantation amounted 16.4 ± 0.1 g, as averaged over 15 mice. (c) Same as panel b, now for the body temperature of the mice. All error bars denote standard deviations over three mice in each group. (For interpretation of the references to colour in this figure legend, the reader is referred to the web version of this article.)

blood markers were all within the range observed for uninfected mice (Table S2). Thus, from the collective data it is concluded that the use of B/C-PEG-cipro/DCPA-H_2O liposomes can be considered to be biosafe.

4. Conclusions

Bromelain-loaded PEG-cipro/DCPA-H_2O liposomes with additional ciprofloxacin loading have been designed. PEG-ciprofloxacin in the lipid membrane of the liposomes acted as a proton sponge, triggering liposome-burst in the acidic environment of an infectious biofilm after self-targeting to a staphylococcal biofilm with the aid of pH-responsive water in DCPA-H_2O. Proton-mediated burst release can also be achieved by other antibiotics such as sulfadiazine, amoxycillin and others, provided they can be PEGylated through a condensation reaction of amino and carboxyl groups. Bromelain loading of such liposomes and its release by proton-mediated liposome-burst degraded the matrix of an infectious biofilm, yielding synergistic action with bacterial killing by ciprofloxacin released in the process of liposome-burst. Notably, due to the controlled, simultaneous release of bromelain and ciprofloxacin, dispersed bacteria were unable to yield septic symptoms in vivo and no adverse effects were observed of the B/C-PEG-cipro/DCPA-H_2O liposomes, paving the way to clinical application. Importantly, with respect to clinical application, bromelain-loaded PEG-cipro/DCPA-H_2O liposomes with additional ciprofloxacin loading are cheap and easy to manufacture and provide a versatile nanocarrier that can also be used for delivery of e.g. chemotherapeutics to an acidic tumor site.

Funding

This work was financially supported by the National Natural Science Foundation of China (51933006). The author thanks to the Dr. Feng, Liu, Dr. Qiji, Shan, Dr. Ling Di and Dr. Mei Gao Shanghai Jiaotong University for her guidance and help in animal experiments.

CRediT authorship contribution statement

Da-Yuan Wang, **Henk. J. Busscher**, and **Linqi Shi** designed experiments. **Da-Yuan Wang**, **Guang Yang** and **Xiao-Xiao Zhang** performed experiments. **Da-Yuan Wang**, **Henk J. Busscher** wrote the manuscript. **Yijin Ren**, **Henk. J. Busscher, Henny C. van der Mei** and **Linqi Shi** edited the manuscript. All the authors analyzed the data and contributed to the paper.

Data and materials availability

All data needed to evaluate the conclusions in the paper are present in the paper and/or the Supplementary Materials. Additional data related to this paper may be requested from the authors.

Declaration of Competing Interest

H.J.B. is also director of a consulting company SASA BV. The authors declare no potential conflicts of interest with respect to authorship and/or publication of this article. Opinions and assertions contained herein are those of the authors and are not construed as necessarily representing views of the funding organization or their respective employer (s).

Data availability

Data will be made available on request.

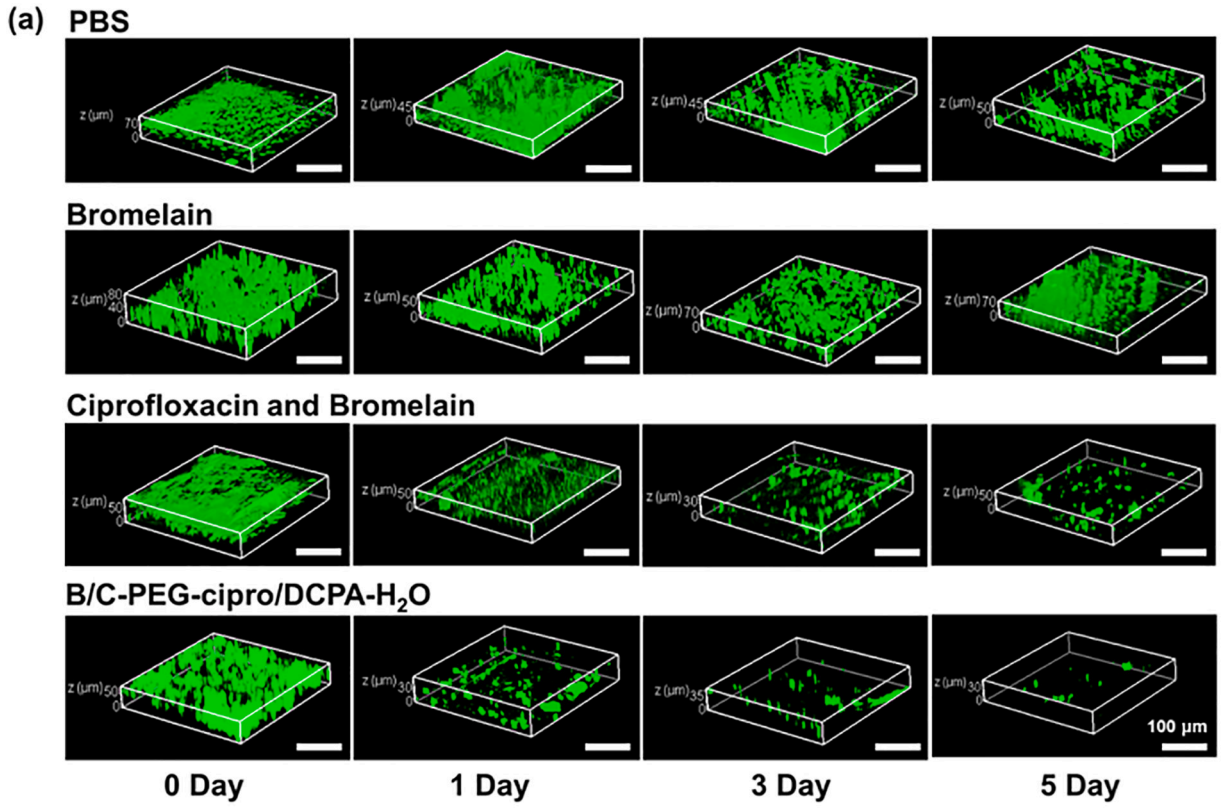

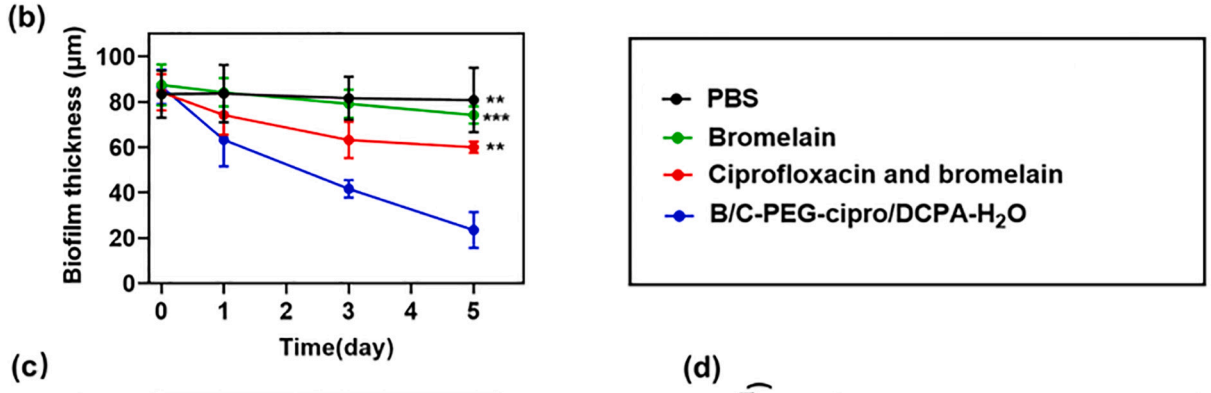

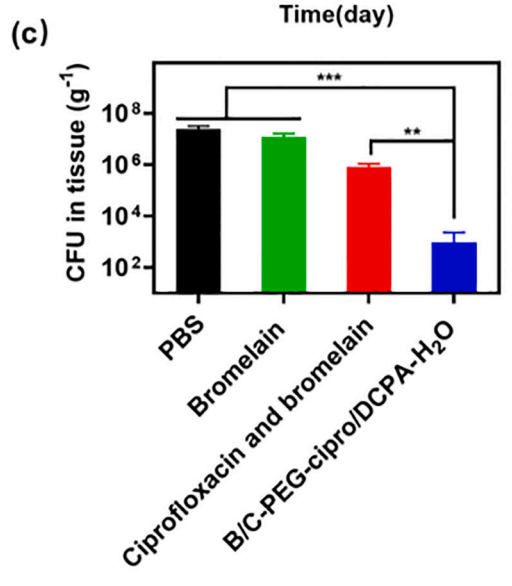

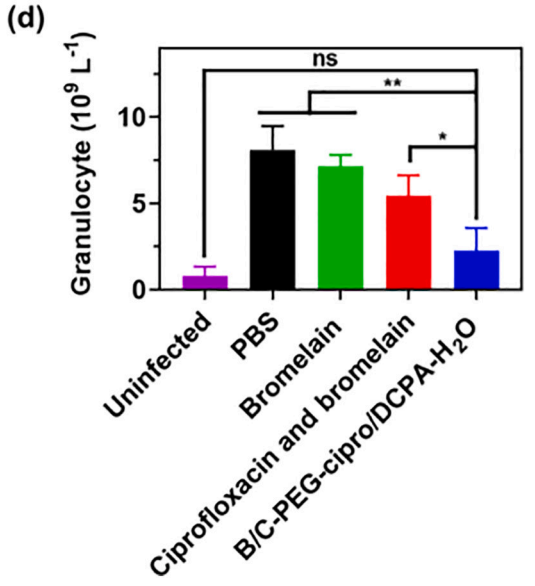

(caption on next page)

Fig. 8. In vivo treatment results of an infectious, *S. aureus* ATCC12600^{GFP} biofilm underneath an abdominal imaging window in mice. (a). Reconstructed 3D intravital images of green-fluorescent *S. aureus* biofilms at different days after starting treatment up to sacrifice at day 5. (b) Thickness of staphylococcal biofilms underneath an abdominal imaging window as a function of time after initiating treatment, derived from COMSTAT analyses [28] of intravital images. (c) Number of *S. aureus* CFUs per g tissue excised from infection site around the abdominal imaging window after sacrifice at day 5. (d) Granulocyte counts in blood of mice in different treatment groups at sacrifice (day 5). All error bars denote standard deviations over three mice in each group. Asterisks indicate statistical significance over comparisons indicated by the spanning bars at $^{*}p < 0.05$, $^{**}p < 0.01$ and $^{***}p < 0.001$ (Students' *t*-test). (For interpretation of the references to colour in this figure legend, the reader is referred to the web version of this article).

Appendix A. Supplementary data

Supplementary data to this article can be found online at https://doi.org/10.1016/j.jconrel.2022.10.049.

References

[1] T. Bjarnsholt, O. Ciofu, S. Molin, et al., Applying insights from biofilm biology to drug development—can a new approach be developed, Nat. Rev. Drug Discov. 12 (10) (2013) 791–808.
[2] D. Fleming, K. Rumbaugh, The consequences of biofilm dispersal on the host, Sci. Rep. 8 (1) (2018) 10738.
[3] A. Bacconi, G. Richmond, M. Baroldi, et al., Improved sensitivity for molecular detection of bacterial and Candida infections in blood, J. Clin. Microbiol. 52 (9) (2014) 3164–3174.
[4] S. Tian, H.C. van der Mei, Y. Ren, et al., Recent advances and future challenges in the use of nanoparticles for the dispersal of infectious biofilms, J. Mater. Sci. Technol. 84 (10) (2021) 208–218.
[5] R. Pavan, S. Jain, Shraddha, et al., Properties and therapeutic application of bromelain: a review, Biotechnol. Res. Int. 2012 (2012), 976203.
[6] L.C. de Lencastre Novaes, A.F. Jozala, A.M. Lopes, et al., Stability, purification, and applications of bromelain: a review, Biotechnol. Prog. 32 (1) (2016) 5–13.
[7] S.J. Taussig, S. Batkin, Bromelain, the enzyme complex of pineapple (*Ananas comosus*) and its clinical application. An update, J. Ethnopharmacol. 22 (2) (1988) 191–203.
[8] C.J. Carter, K. Pillai, S. Badar, et al., Dissolution of biofilm secreted by three different strains of *Pseudomonas aeruginosa* with bromelain, N-acetylcysteine, and their combinations, Appl. Sci. 11 (23) (2021) 11388.
[9] V. Rathnavelu, N.B. Alitheen, S. Sohila, et al., Potential role of bromelain in clinical and therapeutic applications (review), Biomed. Rep. 5 (3) (2016) 283–288.
[10] T. Higashi, T. Kogo, N. Sato, et al., Efficient anticancer drug delivery for pancreatic cancer treatment utilizing supramolecular polyethylene-glycosylated bromelain, ACS Appl. BioMater. 3 (5) (2020) 3005–3014.
[11] M. Zhao, Y. Liu, R.S. Hsieh, et al., Clickable protein nanocapsules for targeted delivery of recombinant p53 protein, J. Am. Chem. Soc. 136 (43) (2014) 15319–15325.
[12] J.V. González-Aramundiz, E. Presas, I. Dalmau-Mena, et al., Rational design of protamine nanocapsules as antigen delivery carriers, J. Control. Release 10 (245) (2017) 62–69.
[13] Y. Jiang, H. Lu, F. Chen, et al., PEGylated albumin-based polyion complex micelles for protein delivery, Biomacromolecules 17 (3) (2016) 808–817.
[14] N. Trac, L.-Y. Chen, A. Zhang, et al., CCR2-targeted micelles for anti-cancer peptide delivery and immune stimulation, J. Control. Release 329 (10) (2021) 614–623.
[15] S. Meyenburg, H. Lilie, S. Panzner, et al., Fibrin encapsulated liposomes as protein delivery system. Studies on the in vitro release behavior, J. Control. Release 69 (1) (2000) 159–168.
[16] Y.B. Kim, K.T. Zhao, D.B. Thompson, et al., An anionic human protein mediates cationic liposome delivery of genome editing proteins into mammalian cells, Nat. Commun. 10 (1) (2019) 2905.
[17] J. Lou, J.A. Schuster, F.N. Barrera, et al., ATP-responsive liposomes via screening of lipid switches designed to undergo conformational changes upon binding phosphorylated metabolites, J. Am. Chem. Soc. 144 (8) (2022) 3746–3756.
[18] A. Jash, A. Ubeyitogullari, S.S.H. Rizvi, Liposomes for oral delivery of protein and peptide-based therapeutics: challenges, formulation strategies, and advances, J. Mater. Chem. B 9 (24) (2021) 4773–4792.
[19] T. Ji, J. Lang, J. Wang, et al., Designing liposomes to suppress extracellular matrix expression to enhance drug penetration and pancreatic tumor therapy, ACS Nano 11 (9) (2017) 8668–8678.
[20] D.-Y. Wang, G. Yang, H.C. van der Mei, et al., Liposomes with water as a pH-responsive functionality for targeting of acidic tumor and infection sites, Angew. Chem. Int. Ed. 60 (32) (2021) 17714–17719.
[21] Y. Liu, L. Shi, L. Su, et al., Nanotechnology-based antimicrobials and delivery systems for biofilm-infection control, Chem. Soc. Rev. 48 (2) (2019) 428–446.
[22] W. Yang, S. Liu, T. Bai, A, et al., Poly(carboxybetaine) nanomaterials enable long circulation and prevent polymer-specific antibody production, Nano Today 9 (1) (2014) 10–16.
[23] A.-H. Ranneh, H. Takemoto, S. Sakuma, et al., An ethylenediamine-based switch to render the polyzwitterion cationic at tumorous pH for effective tumor accumulation of coated nanomaterials, Angew. Chem. Int. Ed. 57 (18) (2018) 5057–5061.
[24] H. Ou, T. Cheng, Y. Zhang, et al., Surface-adaptive zwitterionic nanoparticles for prolonged blood circulation time and enhanced cellular uptake in tumor cells, Acta Biomater. 65 (2018) 339–348.
[25] S. Naik, D. Piwnica-Worms, Real-time imaging of β-catenin dynamics in cells and living mice, Proc. Natl. Acad. Sci. U. S. A. 104 (44) (2007) 17465–17470.
[26] D. Kedrin, B. Gligorijevic, J. Wyckoff, et al., Intravital imaging of metastatic behavior through a mammary imaging window, Nat. Methods 5 (12) (2008) 1019–1021.
[27] S. Tian, L. Su, Y. Liu, J, et al., Self-targeting, zwitterionic micellar dispersants enhance antibiotic killing of infectious biofilms-an intravital imaging study in mice, Sci. Adv. 6 (33) (2020) eabb1112.
[28] K.D. Fugit, B.D. Anderson, The role of pH and ring-opening hydrolysis kinetics on liposomal release of topotecan, J. Control. Release 174 (28) (2014) 88–97.
[29] S. Bersani, M. Vila-Caballer, C. Brazzale, et al., pH-sensitive stearoyl-PEG-poly (methacryloyl sulfadimethoxine) decorated liposomes for the delivery of gemcitabine to cancer cells, Eur. J. Pharm. Biopharm. 88 (3) (2014) 670–682.
[30] H. Chen, H. Zhang, D. Thor, et al., Novel pH-sensitive cationic lipids with linear ortho ester linkers for gene delivery, Eur. J. Med. Chem. 52 (2012) 159–172.
[31] J. Shin, P. Shum, J. Grey, et al., Acid-labile mPEG–vinyl ether–1, 2-dioleylglycerol lipids with tunable pH sensitivity: synthesis and structural effects on hydrolysis rates, DOPE liposome release performance, and pharmacokinetics, Mol. Pharm. 9 (11) (2012) 3266–3276.
[32] D. Chen, K. Sun, H. Mu, et al., pH and temperature dual-sensitive liposome gel based on novel cleavable mPEG-Hz-CHEMS polymeric vaginal delivery system, Int. J. Nanomedicine 7 (2012) 2621–2630.
[33] Q. Chen, H. Ding, J. Zhou, et al., Novel glycyrrhetinic acid conjugated pH-sensitive liposomes for the delivery of doxorubicin and its antitumor activities, RSC Adv. 6 (2016) 17782–17791.
[34] F. Huang, J. Wang, A. Qu, et al., Maintenance of amyloid β peptide homeostasis by artificial chaperones based on mixed-shell polymeric micelles, Angew. Chem. Int. Ed. 53 (34) (2014) 8985–8990.
[35] A. Parodi, S.G. Haddix, N. Taghipour, et al., Bromelain surface modification increases the diffusion of silica nanoparticles in the tumor extracellular matrix, ACS Nano 8 (10) (2014) 9874–9883.
[36] H.-C. Flemming, J. Wingender, U. Szewzyk, et al., Biofilms: an emergent form of bacterial life, Nat. Rev. Microbiol. 14 (9) (2016) 563–575.
[37] H. Wolfmeier, D. Pletzer, S.C. Mansour, et al., New perspectives in biofilm eradication, ACS Infect. Dis. 4 (2) (2018) 93–106.
[38] J.I. Granger, P.-L. Ratti, S.C. Datta, et al., Sepsis-induced morbidity in mice: effects on body temperature, body weight, cage activity, social behavior and cytokines in brain, Psychoneuroendocrinology 38 (7) (2013) 1047–1057.
[39] S.-L. Wang, H.-T. Lin, T.-W. Liang, et al., Reclamation of chitinous materials by bromelain for the preparation of antitumor and antifungal materials, Bioresour. Technol. 99 (10) (2008) 4386–4393.
[40] J.M. Cavaillon, M. Singer, T, Skirecki., Sepsis therapies: learning from 30 years of failure of translational research to propose new leads, EMBO Mol. Med. 12 (4) (2020), e10128.
[41] J. Li, H.J. Busscher, H.C. van der Mei, et al., Surface enhanced bacterial fluorescence and enumeration of bacterial adhesion, Biofouling 29 (1) (2013) 11–19.